

Impact of ICRP-89 Based Models on Dose Estimates for Radiopharmaceuticals and CT Exams

Stabin MG, Kost SD, Clark JH, Pickens DR, Price RR, Carver DE

Vanderbilt University, Nashville, TN, USA

Abstract

New mathematical phantoms based on medical image data are allowing evaluation of internal and external dose calculations using better anatomic realism and inclusion of organs that were not previously defined. In this work, we show preliminary data for new radiation dose estimates for radiopharmaceuticals and CT examinations, using Monte Carlo radiation simulation routines developed in the Geant4 toolkit. Radiopharmaceutical dose estimates show some differences in individual organ dose estimates, but overall very similar effective dose estimates for most radiopharmaceuticals in common use. CT dose estimates now allow for estimation of dose to individual organs as well as accurate effective dose estimates, instead of traditionally available estimates of standard dose to one of two standard sized acrylic phantoms, and, via the use of deformable phantoms, lead to the ability to calculate organ doses and effective doses to more patient-individualized models.

Keywords: Dosimetry, phantoms, Monte Carlo

Introduction

An important update on the mathematical 'phantoms' of the 1980's and 1990's (Figure 1a) (Cristy and Eckerman 1987, Stabin et al. 1995) has been established with the realistic, image based models (Figure 1b) developed by the RADIATION DOSE ASSESSMENT RESOURCE (RADAR) working group of the Society of Nuclear Medicine (Stabin et al. 2009). These models are based on the non-uniform rational b-spline (NURBS) technology developed by Segars (2001), are more realistic than the previous generation models, and also incorporate the updated standard organ masses in Publication 89 of the International Commission on Radiological Protection (ICRP 2003). This 2003 publication supersedes the ICRP's previous publication on this topic (ICRP 1975). Besides a considerable improvement in realism, several new organs were defined that had not been included in previous phantoms, namely the eyes, esophagus, salivary glands and prostate gland. By deforming the original NURBS models to represent adults and children of different ages, a set of male and female reference models were developed, following the age definitions in ICRP 89 (Figure 2), specifically newborns, 1-year-olds, 5-year-olds, 10-year-olds, 15-year-olds, and adults.

RADAR has developed a new version of the OLINDA/EXM software (Stabin et al 2005) that provides several significant updates in technology over previous versions of the code, most importantly the new realistic phantom series for calculation of doses for radiopharmaceuticals. Vanderbilt University has implemented a radiation transport simulation source routine in the GEANT4 Monte Carlo system that models a Computed Tomography (CT) scanner (Figure 3a). The input data for the program represents the energy spectra from one type of CT scanner

(Figure 3b) and various starting and stopping points along the length of the standard examinations given to pediatric subjects. The output of the code provides doses to individual organs, which can be expressed as Effective Dose, applying the appropriate ICRP tissue weighting factors. This can be directly compared to the standard Effective Dose values provided by CT scanners, which are related to 'Dose Length Products', related to dose measurements in 16 or 32 cm acrylic phantoms. Ultimately, our interest is in calculating dose to many pediatric phantoms representing larger and smaller children, obese and non-obese individuals, and other subjects.

In this paper, we shall present radiation doses from radiopharmaceuticals and from CT exams in several subjects using these new realistic phantoms, with direct comparison to currently used models and estimates.

Materials and Methods

A. Radiopharmaceuticals

The principal tool used in this study is the OLINDA/EXM software, as noted above. A new gastrointestinal tract model ('HAT' model) developed by the ICRP (2006) is also implemented in this version of the code. The code includes about 200 new radionuclides, over the approximately 800 in versions 1.0 and 1.1, also based on recently released data of the ICRP (2008a). The previous generation of phantoms is retained in the code, to permit comparisons between the new and old generation of models. The ICRP has also updated its 'tissue weighting factors' for calculation of the quantity 'effective dose' (ICRP 2007); these new weighting factors are included in the code, but two older sets of weighting factors proposed by the ICRP (ICRP 1979, ICRP 1991) are also available for use in the code, again to facilitate comparisons.

Standardized kinetic data for radiopharmaceuticals were taken from the several publications of the ICRP (ICRP 1988, 1998, 2008b) and entered into the OLINDA/EXM 2.0 code, applying appropriate age-dependent values of numbers of disintegrations in urinary bladder, when applicable. Organ doses and effective doses were generated and compared to calculations in version 1.1 of the OLINDA/EXM code and to organ and effective doses given in the ICRP publications.

B. CT Exams

Image sets for several pediatric subjects who had previously undergone CT imaging as part of their routine care at Vanderbilt University were retrieved. A number of identifiable organ regions were manually segmented using the ITK-SNAP toolkit (Yushkevich et al. 2006), as shown in Figure 4. The segmented data were used to score doses in our CT imaging simulation using the Geant4 Monte Carlo toolkit. The simulated CT system uses a fixed number of starting particles

to simulate photon transport and energy deposition in the various defined regions of the segmented models. The starting particles are generated using a photon fluence map, which was created by tracking photons as they exit the collimator of the simulated x-ray tube modeled after our most commonly used pediatric CT scanner (a Philips Brilliance 40). Calibration of the output to absolute dose numbers was achieved by directly exposing CT dosimeters using Optically Stimulated Luminescence (OSL) technology (Figure 5) in an Alderson torso phantom (Alderson et al. 1962). These devices provide profiles of dose across their length; three dosimeters were used with doses averaged over the 3 mm slice width of the scan. The CT image set of the torso phantom was also manually segmented with regions representing the tissue-equivalent rubber material, bone structures, the dosimeters (assumed to be Poly(methyl methacrylate)), and several air spaces in the phantom. A simulation was performed using the segmented phantom, in voxel format, and the resulting dose output in the dosimeter regions used to develop a calibration factor to convert doses in Gy from the Geant simulation to real doses in Gy in physical structures. Several of our male and female NURBS models were voxelized and used in simulations, for comparison to similar pediatric subjects. Effective doses were calculated applying weighting factors from ICRP Publications 60 (1991) and 103 (2007) to the individual organ doses. Computed tomography dose indices (CTDI_s) reported by the CT scanner were listed for comparison. We also calculated ED values from the ImPACT spreadsheet (www.impactscan.org), which were scaled accordingly for pediatric patients.

Results

A. Radiopharmaceuticals

Table 1 shows comparisons of Effective Doses calculated for various pharmaceuticals using the traditional, stylized phantoms and the new, realistic phantoms. In most cases, organ doses are fairly similar, with a few exceptions. Pharmaceuticals that have a high amount of kidney activity will show higher doses to the adrenals, as they are much closer to the kidneys than in the old models. The mass of the pancreas increased from 94.3 g to 140 g, so doses to pancreas tend to be lower. Doses to some organs also will be seen to be higher at times, but when Effective Dose is calculated, applying weighting factors to many target organs, some of which have slightly higher doses, some which have slightly lower doses, and some that have not changed significantly, the overall effect is small.

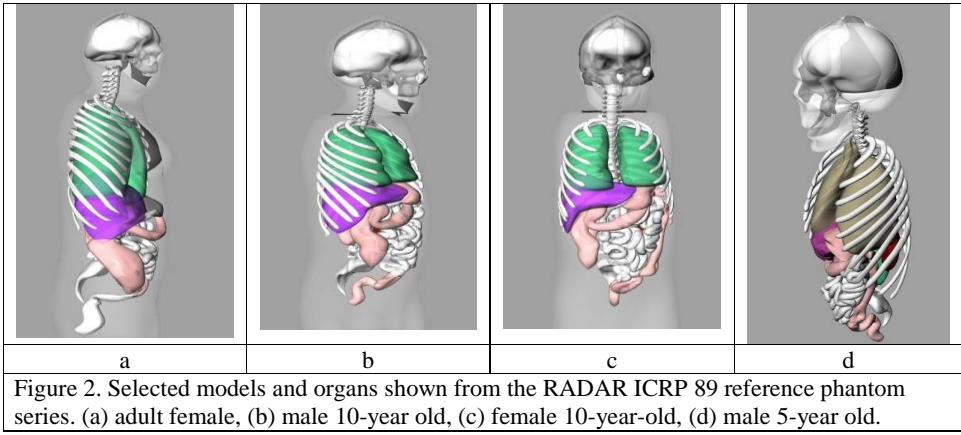
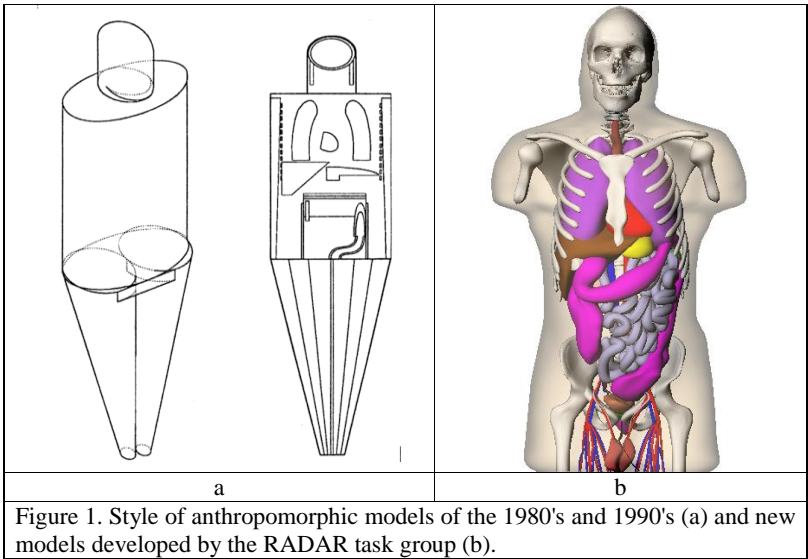
B. CT Exams

Patient demographics and examination details for the patients receiving CT examinations are shown in Table 2. Dose estimates for selected organs for these patients, with comparison to CTDI and ED values, are shown in Table 3. Dose estimates for selected organs of the NURBS models and ED values are shown in Table 4, with comparison to a chosen real pediatric patient based on similar ages and effective diameters.

Discussion

The new generation of anthropomorphic phantoms clearly represents a significant improvement in anatomic realism - organs are more explicitly modeled, and the proximity of organs is better modeled. Organs are closer together, and many are in direct contact with each other (kidneys/adrenals, lungs/heart), whereas in stylized models, separation of organ spaces occurs due to the simplicity of the shapes employed to model them. Changes in actual SAF values from the Cristy/Eckerman model series were seen, but were mostly small in magnitude. The impact on calculated dose estimates for radiopharmaceuticals, as shown in Table 1, are minor. The availability of newly defined organs (esophagus, salivary glands, eyes, prostate) results in improved estimates of effective dose.

The use of the NURBS models with simulated CT sources permits the calculation of individual organ doses and effective doses. This also is a significant improvement over the use of quantities like DLP to estimate radiation doses. Table 3 shows significant differences in calculated ED values for the different subjects, while the DLP values are generally similar. Comparisons of ED values between NURBS models and similar pediatric subjects (Table 4) were favorable and may be improved with better matching criteria.



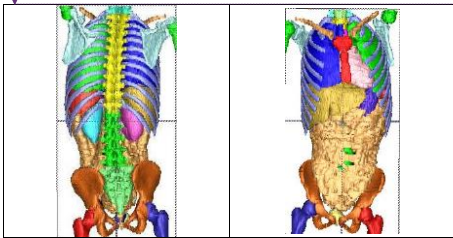


Figure 4. Segmented organs in 9-year-old female patient (Subject11 in Table 2).



Figure 5. Optically Stimulated Luminescence (OSL) CT dosimeters © Landauer, Inc.

Deleted: ¶

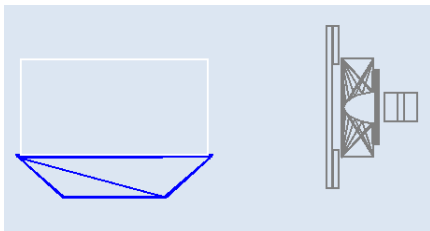


Figure 3a. Graphic representation of the rotating CT source created in the GEANT4 environment for estimation of CT doses to subjects. The CT head is at the right, the trapezoidal structure at the bottom is the imaging table and the rectangular space above is where voxelized patient structures are located.

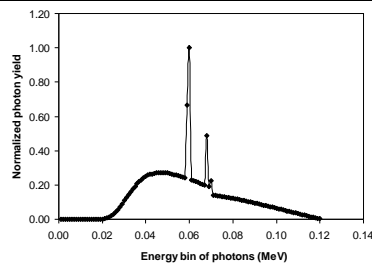


Figure 3b. Photon energy spectrum generated by the GEANT4 source module, using 120 keV electrons as the source.

Table 1. Comparison of Effective Doses (mSv/MBq administered) for selected radiopharmaceuticals for five reference phantoms.

		Adult	15-yr	10-yr	5-yr	1-yr
18FDG	Old	1.86E-02	2.39E-02	3.58E-02	5.29E-02	8.90E-02
	New	1.73E-02	2.21E-02	3.26E-02	4.76E-02	7.83E-02
	Ratio	9.30E-01	9.25E-01	9.11E-01	9.00E-01	8.80E-01
11C Acetate	Old	3.03E-03	3.77E-03	5.70E-03	8.60E-03	1.59E-02
	New	2.88E-03	3.72E-03	5.41E-03	8.20E-03	1.38E-02
	Ratio	9.50E-01	9.87E-01	9.49E-01	9.53E-01	8.68E-01
99mTc MAA	Old	1.17E-02	1.64E-02	2.35E-02	3.54E-02	6.56E-02
	New	1.10E-02	1.40E-02	2.21E-02	3.31E-02	5.85E-02
	Ratio	9.40E-01	8.54E-01	9.40E-01	9.35E-01	8.92E-01
111In Octreotide	Old	5.15E-02	6.76E-02	1.01E-01	1.49E-01	2.42E-01
	New	5.09E-02	6.34E-02	9.19E-02	1.30E-01	2.02E-01
	Ratio	9.88E-01	9.38E-01	9.10E-01	8.72E-01	8.35E-01
12I BMIPP	Old	1.51E-02	1.92E-02	2.94E-02	4.44E-02	8.05E-02
	New	1.49E-02	1.94E-02	2.79E-02	4.08E-02	7.13E-02
	Ratio	9.87E-01	1.01E+00	9.49E-01	9.19E-01	8.86E-01

Table 2. Patient demographics and examination details for pediatric subjects receiving CT examinations

Subject No.	Age, gender	Exam type	mAs	pitch
1	6 mo male	CAP	100	1.176
2	1 yo male	CAP	100	1.176
3	2 yo male	CAP	100	1.176
4	4 yo male	CAP	107	0.924
5	5 yo male	CAP	75	0.924
6	6 yo male	CAP	110	0.906
7	8 yo male	CAP	117	1.176
8	8 yo male	CAP	88	0.924
9	10 mo female	AP	60	1.176
10	4 yo female	CAP	110	0.906
11	9 yo female	CAP	180	0.906
12	14 yo female	CAP	160	1.077

All studies: 120 kVp. CAP=Chest/Abdomen/Pelvis, AP=Abdomen/Pelvis

Table 3. Doses to selected organs and effective doses for pediatric subjects receiving CT examinations

Subject	Organ doses (mGy) and Effective Doses (mSv)					
	1	2	3	4	5	6
Adrenals	12.5	10.5	11.2	15.1	10.6	13.4
Bone/marrow	25.5	23.9	23.7	31.8	20.9	30.1
Esophagus	11.1	10.3	10.5	14.6	10.4	13.8
Intestine	12.8	11.5	8.9	16.4	11.0	16.0
Kidneys	12.6	11.3	12.0	15.7	11.0	15.8
Liver	12.1	11.4	11.4	15.1	11.0	15.4
Lungs	12.4	11.4	11.6	15.8	11.3	15.3
Stomach	12.9	11.4	11.4	16.5	11.1	15.6
Spleen	12.4	11.0	12.1	16.4	11.0	14.9
Thymus	11.5	11.0	10.8	14.6	10.4	15.1
Thyroid	8.7	9.5	9.4	12.2	7.6	13.0
CTDI _{vol}	7	7	7	7.49	5.3	6.5
ED ICRP 60	10.5	9.6	9.4	13.3	8.9	12.7
ED ICRP 103	10.6	9.7	9.5	13.4	9.0	12.8
CTDI _{vol}	7.0	7.0	7.0	7.5	6.5	6.5
ImPACT scaled ED	17.2	15.8	14.6	18.7	12.3	15.8

Subject	Organ doses (mGy) and Effective Doses (mSv)					
	7	8	9	10	11	12
Adrenals	10.5	10.3	3.5	15.8	23.4	13.9
Bone/marrow	23.1	22.8	1.8	33.3	51.4	27.2
Esophagus	10.9	10.8	2.3	14.8	22.5	12.9
Intestine	11.8	11.9	3.0	17.1	24.0	14.8
Kidneys	11.8	11.4	3.2	16.7	25.6	15.3
Liver	12.0	12.1	3.7	16.2	24.1	15.9
Lungs	12.1	12.1	9.0	15.8	24.6	14.3
Stomach	11.7	11.7	3.3	17.2	23.9	16.1
Spleen	11.5	11.2	3.6	15.0	23.2	14.9
Thymus	11.1	12.0	0.0	14.9	0.0	13.1
Thyroid	10.2	8.5	0.0	15.6	23.2	0.0
CTDI _{vol}	8.19	6.2	4.2	6.5	10.6	11.2
ED ICRP 60	12.0	9.6	2.5	14.0	24.4	14.5
ED ICRP 103	10.8	9.7	2.6	14.2	22.1	14.4
CTDI _{vol}	8.2			6.5	10.6	11.2

ImPACT scaled ED	14.3	13.7	7.1	16.8	23.2	15.4
------------------	------	------	-----	------	------	------

Table 4. Doses to selected organs and effective doses for NURBS models, with comparison to selected pediatric patient data

	Organ doses (mGy) and Effective Doses (mSv)			Organ doses (mGy) and Effective Doses (mSv)		
	10-yo female phantom	9-yo female patient	Ratio	15-yo female phantom	14-yo female patient	Ratio
Adrenals	25.0	23.4	0.94	13.7	13.9	1.01
Brain	4.1	4.0	0.99	2.5	1.9	0.74
Esophagus	26.0	22.5	0.86	14.3	12.9	0.90
Intestine	25.0	24.0	0.96	13.9	14.8	1.06
Heart	27.6	27.4	0.99	19.8	14.7	0.74
Kidneys	26.1	25.6	0.98	14.4	15.3	1.06
Liver	26.5	24.1	0.91	14.7	15.9	1.08
Lungs	28.0	24.6	0.88	15.6	14.3	0.92
Stomach	26.6	23.9	0.90	14.6	16.1	1.10
Spleen	26.1	24.0	0.92	14.6	14.9	1.02
ED ICRP 60	25.72	23.51	0.91	14.20	14.55	1.02
ED ICRP 106	25.02	21.52	0.86	14.07	14.50	1.03

	Organ doses (mGy) and Effective Doses (mSv)			Organ doses (mGy) and Effective Doses (mSv)		
	5-yo male phantom	5-yo male patient	Ratio	5-yo male phantom	6-yo male patient	Ratio
Adrenals	9.5	10.6	1.12	14.2	13.4	0.94
Brain	2.3	0.9	0.41	2.3	1.4	0.61
Esophagus	9.4	10.4	1.10	14.1	13.8	0.98
Intestine	10.0	11.0	1.10	14.9	16.0	1.07
Heart	27.0	11.0	0.41	27.0	16.4	0.61
Kidneys	9.9	11.0	1.11	14.8	15.8	1.07
Liver	10.0	11.0	1.10	14.9	15.4	1.03
Lungs	10.6	11.3	1.07	15.8	15.3	0.97
Stomach	10.0	11.1	1.11	14.9	15.6	1.05
ED ICRP 60	9.35	9.04	0.97	14.0	12.6	0.90
ED ICRP 106	9.34	9.86	1.06	14.0	13.7	0.98

References

Alderson SW, Lanzl LH, Rollins M, and Spira J. An instrumented phantom system for analog computation of treatment plans. *American Journal of Roentgenology, Radium Therapy and Nuclear Medicine*, 87, 185-195, 1962.

Cristy M, Eckerman K. Specific absorbed fractions of energy at various ages from internal photons sources. ORNL/TM-8381 V1-V7, Oak Ridge National Laboratory, Oak,Ridge, TN, 1987.

International Commission on Radiological Protection: Report of the Task Group on Reference Man, ICRP Publication 23, Pergamon Press, New York, NY, 1975.

International Commission on Radiological Protection. Limits for Intakes of Radionuclides by Workers. ICRP Publication 30, Pergamon Press, New York, 1979.

International Commission on Radiological Protection. Radiation Dose to Patients from Radiopharmaceuticals. ICRP Publication 53. *Ann. ICRP* 18 (1-4), 1988.

International Commission on Radiological Protection. 1990 Recommendations of the International Commission on Radiological Protection. ICRP Publication 60, Pergamon Press, New York, 1991.

International Commission on Radiological Protection. Radiation Dose to Patients from Radiopharmaceuticals (Addendum to ICRP Publication 53). ICRP Publication 80. *Ann. ICRP* 28 (3), 1998.

International Commission on Radiological Protection. ICRP Publication 89: Basic Anatomical and Physiological Data for Use in Radiological Protection: Reference Values, Elsevier Health, 2003.

International Commission on Radiological Protection. Human Alimentary Tract Model for Radiological Protection. ICRP Publication 100. *Ann. ICRP* 36 (1-2), 2006

International Commission on Radiological Protection. 2007 Recommendations of the International Commission on Radiological Protection (Users Edition). ICRP Publication 103 (Users Edition). *Ann. ICRP* 37 (2-4), 2007.

International Commission on Radiological Protection. Nuclear Decay Data for Dosimetric Calculations. ICRP Publication 107. *Ann. ICRP* 38 (3), 2008.

International Commission on Radiological Protection. Radiation Dose to Patients from Radiopharmaceuticals - Addendum 3 to ICRP Publication 53. ICRP Publication 106. *Ann. ICRP* 38 (1-2), 2008.

Segars JP. Development and Application of the New Dynamic NURBS-based Cardiac-Torso (NCAT) Phantom, Ph.D. Dissertation, The University of North Carolina, 2001.

Stabin MG, Emmons-Keenan MA, Segars WP, Fernald MJ. The Vanderbilt University Reference Adult and Pediatric Phantom Series. *Handbook of Anatomical Models for Radiation Dosimetry*, CRC Press, Boca Raton, FL, 2009, pp 337-346.

Stabin MG, Sparks RB, Crowe E. OLINDA/EXM: The Second-Generation Personal Computer Software for Internal Dose Assessment in Nuclear Medicine. *J Nucl Med* 2005;46 1023-1027.

Stabin M., Watson E., Cristy M., Ryman J., Eckerman K., Davis J., Marshall D., Gehlen K. Mathematical models and specific absorbed fractions of photon energy in the nonpregnant adult female and at the end of each trimester of pregnancy. ORNL Report ORNL/TM-12907, 1995.

Yushkevich PA, Piven J, Hazlett HC, Smith RG, Ho S, Gee JC, Gerig G. User-guided 3D active contour segmentation of anatomical structures: Significantly improved efficiency and reliability. *Neuroimage* 2006 Jul 1;31(3): 1116-28.